Electrocorticography is superior to subthalamic local field potentials for movement decoding in Parkinson's disease

Timon Merk[1], Victoria Peterson[2,5], Witold Lipski[3], Benjamin Blankertz[4], Robert S. Turner[3], Ningfei Li[1], Andreas Horn[1], R. Mark Richardson[2,5]*, Wolf-Julian Neumann[1]*

[1]Movement Disorder and Neuromodulation Unit, Department of Neurology, Charité – Universitätsmedizin Berlin, Berlin, Berlin, 10117, Germany
[2]Brain Modulation Lab, Department of Neurosurgery, Massachusetts General Hospital, Boston, Massachusetts, 02114, USA
[3]Department of Neurobiology, University of Pittsburgh, Pittsburgh, Pennsylvania, 15213, USA
[4]Department of Computer Science, Technische Universität Berlin, Berlin, Berlin, 10587, Germany
[5]Harvard Medical School, Boston, Massachusetts, 02114, USA

*These authors contributed equally to this work

Corresponding author and Lead contact: Wolf-Julian Neumann, MD, Assistant Professor for Interventional and Cognitive Neuromodulation, Movement Disorder and Neuromodulation Unit, Charité – Universitätsmedizin Berlin, Chariteplatz 1, 10117 Berlin, julian.neumann@charite.de

Email:
Timon Merk: timon.merk@charite.de
Victoria Peterson: vpeterson2@mgh.harvard.edu
Witold Lipski: lipskiw@upmc.edu
Benjamin Blankertz: benjamin.blankertz@tu-berlin.de
Robert Sterling Turner: rturner@pitt.edu
Ningfei Li: Ningfei.li@charite.de
Andreas Horn: andreas.horn@charite.de
Robert Mark Richardson: Mark.Richardson@mgh.harvard.edu
Wolf-Julian Neumann: julian.neumann@charite.de

Author Contributions:
Conceptualization, T.M., R.M.R. & W.J.N.;
Methodology, T.M., V.P., W.L., A.H., R.M.R., W.J.N.;
Software, T.M., V.P., A.H., N.L., W.J.N.;
Validation, W.J.N.;
Formal Analysis, T.M. & V.P.;

Abstract

Brain signal decoding promises significant advances in the development of clinical brain computer interfaces (BCI). In Parkinson's disease (PD), first bidirectional BCI implants for adaptive deep brain stimulation (DBS) are now available. To elevate the therapeutic potential of BCI with machine learning, further research is required to characterize optimal recording sources, computational methods and interactions of pathophysiology and decoding performance. Here, we developed an invasive brain-signal decoding approach based on sensorimotor electrocorticography (ECoG) and subthalamic LFP to predict grip-force in 11 PD patients. We compare decoding performances across signal modalities, investigate the role of PD motor impairment and elucidate a relationship of whole-brain connectivity and model performance. We demonstrate that ECoG is superior to subthalamic LFP for accurate grip-force decoding. Performance negatively correlated with PD motor impairment, suggesting that pathophysiology can restrict the neural capacity to encode movement kinematics. Using connectomic fingerprints of the sensor locations and their connectivity profiles, allowed to predict grip-force decoding performance of individual sensors across patients. In conclusion, our study provides a neurophysiological and computational framework for invasive brain signal decoding to aid the development of an individualized precision-medicine approach to intelligent adaptive DBS.

Keywords

Parkinson's disease, Deep brain stimulation, Machine learning, Neuromodulation, Basal ganglia

Significance Statement

Neurotechnology will revolutionize the treatment of neurological and psychiatric patients, promising novel treatment avenues for previously intractable brain disorders. However, optimal surgical and computational approaches and their interactions with neurological disorders are unknown. How can recent advances in machine learning and connectomics aid the precision and performance of invasive brain signal decoding strategies? Do the brain disorders treated with such approaches have impact on decoding performance? We propose a real-time compatible advanced machine learning pipeline for invasively recorded brain signals in Parkinson's disease (PD) patients. We report optimal movement decoding strategies with respect to signal source, model architecture and connectomic fingerprint and investigate impact of PD motor impairment on applied grip-force as a relevant kinematic target variable for movement decoding.

Introduction

Subthalamic deep brain stimulation (DBS) for Parkinson's disease (PD) is one of the most successful neurotechnological advances in translational neuroscience to date. In addition to its clinical utility, DBS has provided unique insight into the neurophysiology of movement disorders .(Cagnan et al., 2019; Krauss et al., 2021) Here, PD has been associated with increased beta synchronization in the basal ganglia(Kehnemouyi et al., 2021; Kühn et al., 2006; Neumann et al., 2016) and exaggerated phase amplitude coupling and waveform sharpness asymmetry in cortex.(Cole et al., 2017; de Hemptinne et al., 2015) Symptom severity in the OFF medication state was shown to correlate with resting beta power in the STN across patients.(Kühn et al., 2006; Neumann et al., 2016) Such observations have inspired the idea of adaptive DBS (aDBS), where electrophysiological signals are used to change stimulation parameters in response to evolving clinical states.(Beudel and Brown, 2016; Hwang et al., 2020; Little et al., 2013; Petrucci et al., 2020; Piña-Fuentes et al., 2019; Swann et al., 2018; Tinkhauser et al., 2017; Velisar et al., 2019) In a series of seminal papers it was shown that significant clinical benefit and reduced side-effects could be achieved, when stimulation was triggered by beta power.(Little et al., 2013; Velisar et al., 2019)

Machine-learning for aDBS applications can integrate multivariate feature sets for adaptive DBS control beyond beta power. First trials on machine learning based movement classification to trigger adaptive DBS either using electrocorticography (ECoG) or subcortical local field potentials (LFP) in essential tremor have shown promising results.(He et al., 2021; Opri et al., 2020) Given the well described relationship of vigor, movement velocity, bradykinesia and dopamine,(Lofredi et al., 2018; Turner and Desmurget, 2010; Yttri and Dudman, 2016) we speculate that decoding of grip-force as an indirect surrogate of vigor in PD holds relevance for the future development of adaptive DBS algorithms in PD. Here, detection of vigorous movements may trigger an increase of stimulation amplitude, helping to counteract the loss of movement amplitude and velocity through bradykinesia. Moreover, decoding of grip-force can serve as an experimental paradigm for further refinement of neurophysiological and computational tools for brain signal decoding in DBS patients. In the present study we aimed at decoding continuous *grip-force* by combining state-of-art machine learning algorithms with multimodal invasive neurophysiology and whole-brain connectomics in PD patients. Our results address the utility of cortical vs. subcortical signals to accurately decode grip-force and establish a link between decoding performance and motor impairment in PD. Finally, machine learning performance of cortical recording locations could be predicted based on structural and functional connectivity fingerprints seeding from recording locations. Together, this multimodal connectomic decoding framework will impact BCI implant strategies beyond movement disorders.

Results

Real-time processing & Feature Definition

We analyzed sensorimotor ECoG and subthalamic LFP data recorded intraoperatively during performance of a grip force task from 11 patients with PD, undergoing DBS implantation (Figure 1A). Individual electrode localizations in montreal neurological institute (MNI) space are shown in Figure 1B with typical

responses(Androulidakis et al., 2007; Kondylis et al., 2016; Kühn et al., 2004; Lofredi et al., 2018) in Figure 1C aligned to onset of grip force (total n=2685, on average n=244 ± 149 STD trials per patient). For the use in machine learning models, band power feature time-series were extracted in a real-time BCI compatible implementation (Figure 1D) streamed in virtual packets of 100 ms length at a sampling rate of 1000 Hz to mimic the online application. Variance as a measure of amplitude of rereferenced, band-pass filtered raw data segments was extracted at 10 Hz with an adaptive window length from 1000 – 100 ms of past data for eight oscillatory features [θ (4-8 Hz), α (8-12 Hz), β (13-35 Hz), low β (13-20 Hz), high β (20-35 Hz), all γ (60-200 Hz), γ (60-80 Hz) and high frequency activity (HFA) (90-200 Hz)]. All features were normalized to the median of the past 10 seconds to ensure sustainable performance. The target variable was the continuously measured grip-force (z-scored for each recording session), which was cleaned from noise and baseline drift.(Xie et al., 2018)

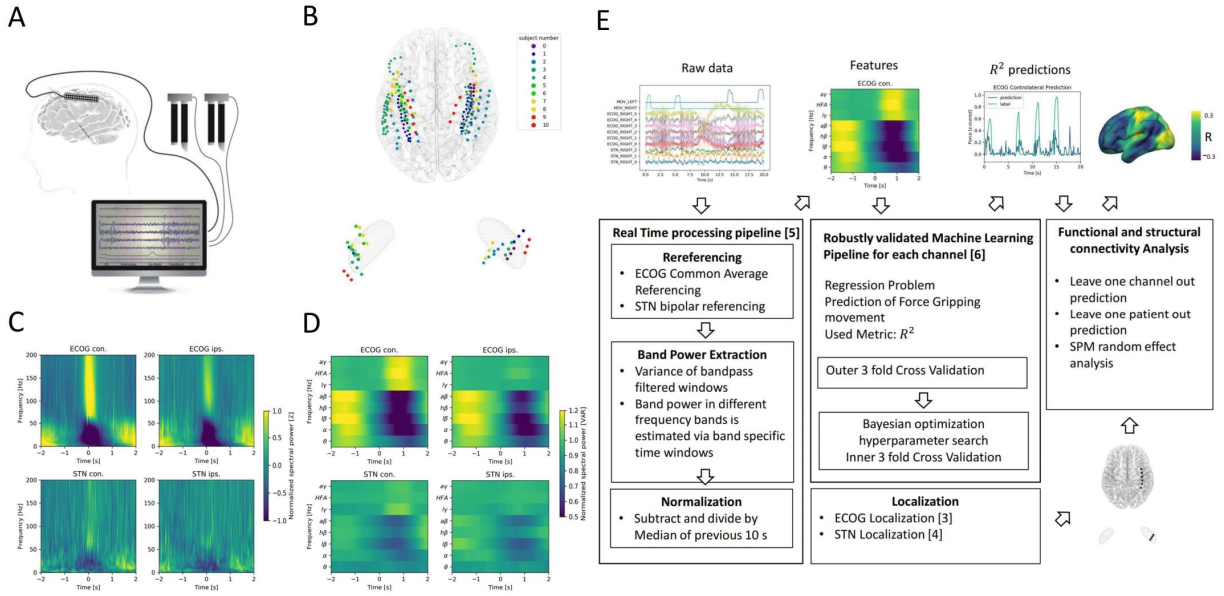

Figure 1: Movement induced spectral changes are more dominant for ECoG than STN-LFP signals for a grip force task before and after a machine learning feature signal processing pipeline. (A) ECoG, STN and gripping force were recorded simultaneously. (B) Individual ECoG and STN electrodes were localized (and transformed into) in Montreal Neurological Institute (MNI) space. Note that ECoG strip designs varied slightly between patients, leading to varying dimensions of overall input feature matrices. The number of ECoG channels (average n= 9.45 ± 11.15 STD per hemisphere) is higher compared to the number of STN LFP channels (n=3). (C) Mean spectral power of all ECoG and STN channels for contra - and ipsilateral movements showed typical movement induced spectral changes. (D) Virtual streaming of data packets secured real-time compatible processing and normalization to extract time-frequency modulations into discrete feature time-series. Mean features of all EcoG and STN channels are visualized. (E) Schematic flow chart of the implemented real-time enabled feature extraction, machine learning evaluation and functional and structural connectivity analysis pipeline.

Performance saturation occurs at a time concatenation of 500 ms

A linear model analysis of all eight oscillatory features per channel was used to investigate the resulting contributing band correlations for time-points preceding target samples of continuous grip-force measurements. Figure 2A shows average weight distributions for the best performing channels per electrode (Figure 2B). Next, to investigate the cumulative performance contribution of previous time points for optimal feature construction, all frequency bands were concatenated while continuously increasing the cumulative number of premovement time-points (from -100 to -1000 ms) and each set trained as a Wiener Filter. The respective best channel R^2 performances are shown in Figure 2C. A performance saturation becomes visible when concatenating 5 time-points from 500 ms (prior to target sample) to 0 ms (target sample), resulting in an optimal input vector of 8 frequency bands with 5 time-points (= 40 features) for further analyses.

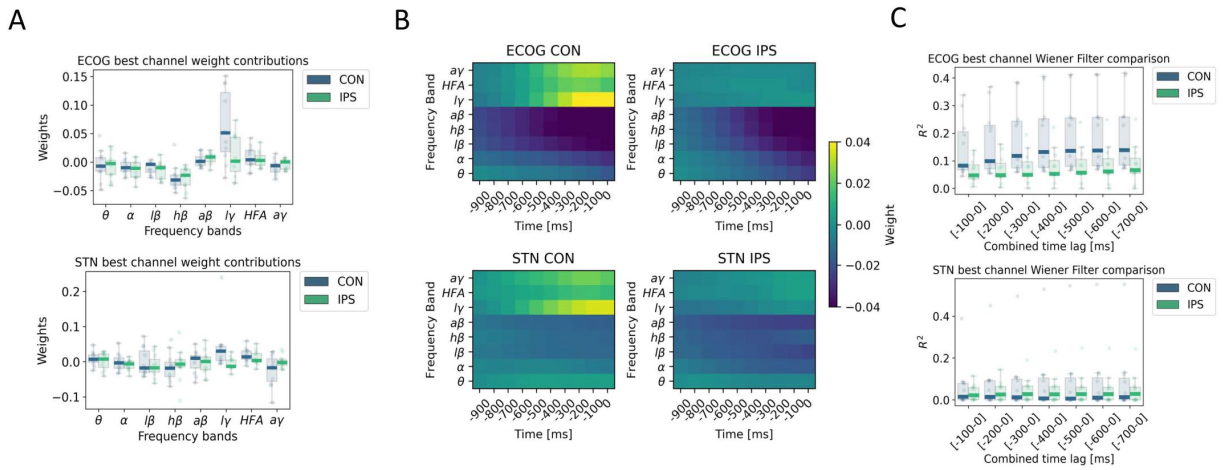

Figure 2: Linear Model analysis shows movement typical frequency band coefficients and linear Wiener Filter performance comparison show performance gain of concatenated features with a lag up to 500 ms. (A) Best patient specific linear model coefficients show movement induced spectral changes, with stronger deflection for ECoG than STN-LFP signals. (B) Individual frequency band and time shifted Linear Model coefficients reveal movement specific feature importance. *HFA* and γ bands show stronger deflection for contralateral over ipsilateral movements. Moreover, stronger deflections are visible for ECoG over STN-LFP signals for β, *HFA* and γ bands. (C) Linear Wiener Filters of cumulative time-points demonstrate performance gain of concatenated features from -500 ms prior to the target sample up to 0 ms (target sample of grip-force measure) for ECoG and STN-LFP signals.

XGBOOST regression shows highest decoding performance for grip-force prediction

In order to build a grip-force decoder, different machine learning (ML) algorithms were tested in a large-scale Bayesian Optimization hyperparameter search. Elastic-net regularized Linear Models, Neural Networks and Gradient Boosted trees (XGBOOST)(Chen and Guestrin, 2016) were tested for each channel for contra- and ipsilateral movements. XGBOOST was tested to learn non linearities and perform an optimal

selection of features. To further utilize potential information derived from spatial patterns, the Source Power Comodulation (SPoC) framework(Dähne et al., 2014) was used in combination with elastic-net or XBGOOST predictors. Each model was informed by 40 features (8 specific frequency bands concatenated at 5 time-points ranging from t = -500 ms to t = 0 ms to the target sample) per channel and evaluated via rigorously cross-validated test-set predictions using R^2 coefficients of determination.

Figure 3 shows performance outcomes for the different machine learning methods, with overall best results achieved by XGBOOST. Decoding performances from contralateral ECoG strips show statistical significance over ipsilateral ones (contralateral R^2=0.31±24, ipsilateral R^2=0.13±0.16, p-value=0.02). ECoG XGBOOST performances showed higher performance differences to other ML methods for contralateral movements (Table S2). ECoG performances increased when the complexity of the machine learning algorithms increased, while STN performances saturated regardless of model complexity. Given the relatively low decoding performances for STN-LFP, we applied permutation tests to confirm that performance was above chance (contralateral p=0.025, ipsilateral p=0.028). Corroborating the model choice in previous literature, highest STN performances were achieved with the Wiener Filter method for contra - and ipsilateral movements.(Shah et al., 2018) Importantly, varying combinations of multiple ECoG and/or STN channels did not lead to significant performance advantages (Figure 4B), which is important for the utility and design of machine learning capable implantables.

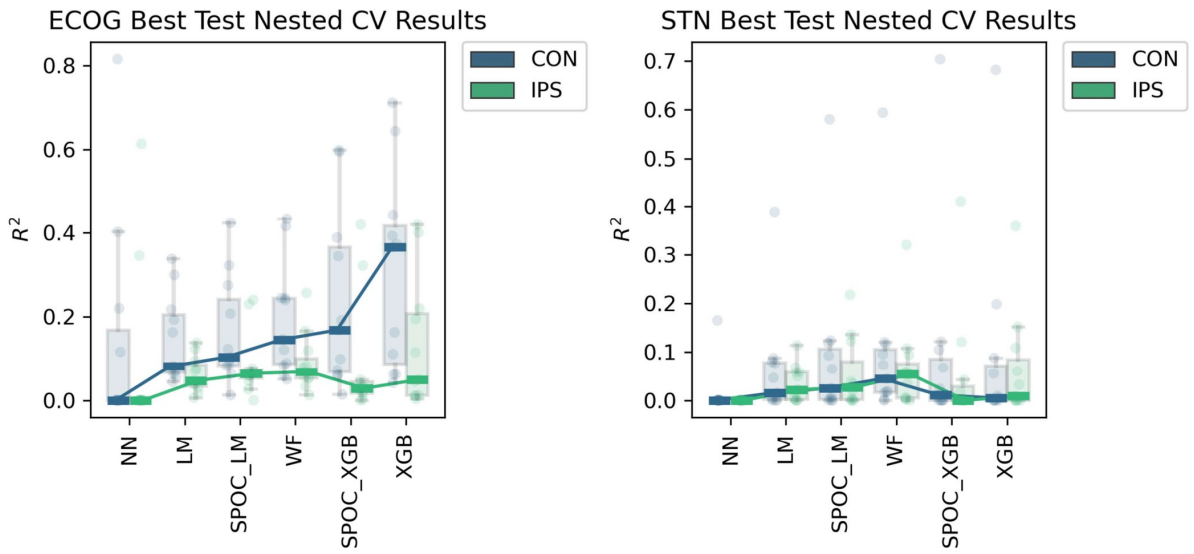

Figure 3: XGBOOST regression shows highest movement decoding performance as compared to other machine learning methods. Based on the presented real-time compatible signal processing pipeline Elastic Net regularized Linear Models (LM) and Wiener Filters (WF), Neural Networks (NN) and extreme Gradient Boosting (XGBOOST) regression was tested. Mean R^2 performances are shown for the best patient specific channel of optimal Bayesian Optimization obtained hyperparameters. The same pipeline was applied for a spatial feature approach using all available channels of an electrode for each patient with Source Power Comodulation (SPoC). Best ECoG performances were obtained by XGBOOST regressors.

STN-LFP signals did not exhibit performance gain when applying advanced machine learning methods. The mean ECoG minus STN XGBOOST performance differences of contralateral ΔR^2= 0.21 ± 0.18 and ipsilateral ΔR^2= 0.069 ± 0.08 movements, indicate the higher grip-force decoding performance of ECoG over STN signals. Throughout every patient the mean test set prediction performances were higher for ECoG than for STN, for both contra -and ipsilateral movements.

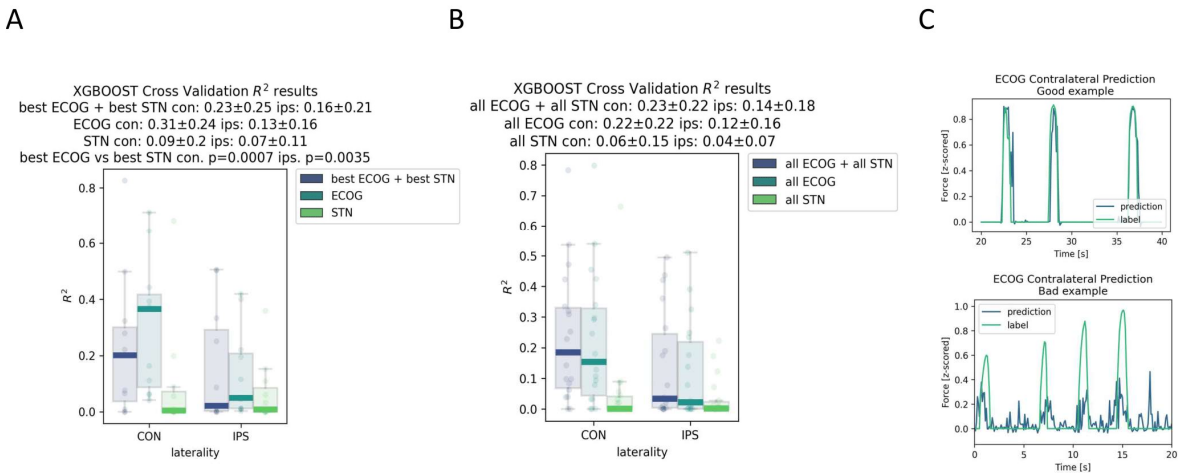

Figure 4: ECoG decoding performance significantly outperforms STN-LFP decoding performance. (A) Individual best XGBOOST decoding performances show throughout every patient performance gain of ECoG over STN-LFPs (contralateral p-value=0.0007, ipsilateral p-value=0.035). (B) When combining multiple channels, best performances are achieved with combined ECoG and STN-LFPs, but performance remains below individual best ECoG as depicted in (A). For ECoG and STN combined features, the model learned specific combinations between both feature locations and failed to select ECoG only due to overfitting. (C) Exemplary good and poor test set predictions of individual ECoG contralateral and ground truth grip-force traces.

Decoding performance is correlated with PD motor impairment

Furthermore, we tested for potential explaining variables of decoding performance using Spearman's correlation. Age (ρ = -0.16, p-value=0.32), disease duration in years (ρ = 0.31, p-value=0.17) and number of movements (ρ = -0.41, p-value=0.11) did not show significant correlation to mean all channel contra -and ipsilateral decoding performance. To test for motor impairment related to the hypodopaminergic state in PD, we used preoperative OFF medication scores. Total UPDRS-III scores showed negative correlation to the patient wise mean of contra -and ipsilateral performances for ECoG (ρ = -0.55, p-value=0.043) and STN (ρ = -0.55, p-value=0.039) channels (Figure 5A+B). Combined ECoG and STN channel performance also showed significant correlation (ρ = -0.54, p-value=0.045), as well as combined ECoG (ρ = -0.55, p-value=0.045) and combined STN (ρ = -0.61, p-value=0.024). To test whether the correlation measure was corrupted by outliers, we repeated the analysis using the robust percentage-bend correlation, (Pernet et al., 2013) which showed a significant association between UPDRS total score and mean contra -and ipsilateral channel performance for ECoG (r = -0.62, p-value=0.04) and STN (r = -0.7, p-value=0.016). This correlation was temporally specific to decoding of ongoing grip-force, indicative of the models' underestimation of motor output (Figure 5C). This has practical implications and highlights the importance of investigating interactions between disease and machine learning approach for neural implants.

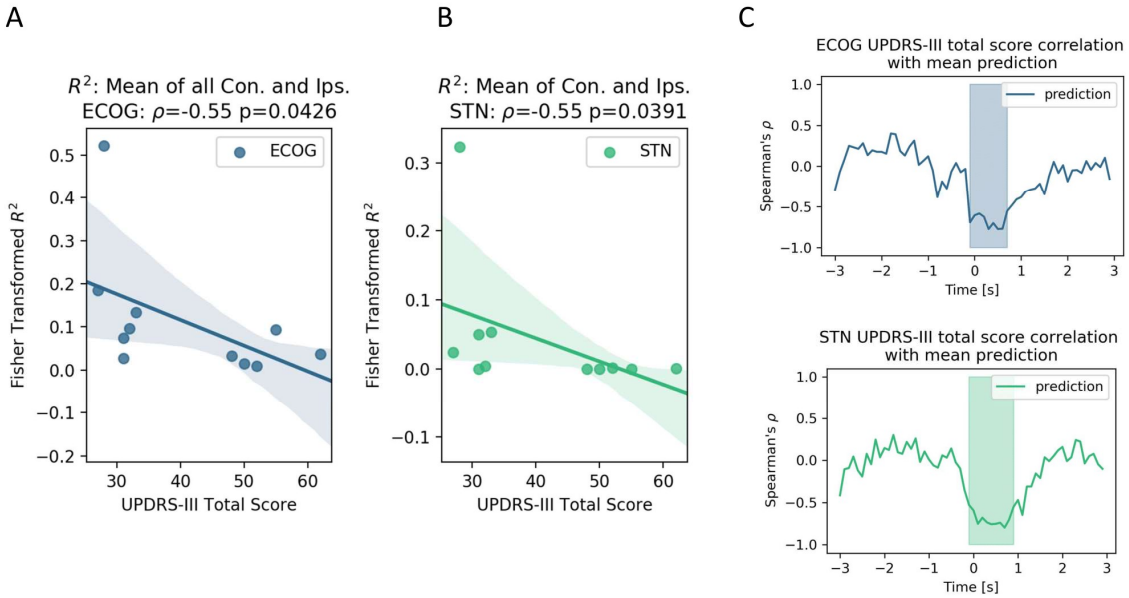

Figure 5: Individual patient XGBOOST R^2 performances show negative PD UPDRS-III clinical symptom severity correlation. UPDRS-III scores show significant negative correlation to mean contra- and ipsilateral channels for (A) ECoG (ρ = -0.55, p-value=0.0426) and (B) STN performances (ρ = -0.55, p-value=0.039). Mean contra -and ipsilateral performances are used, since UPDRS-III total scores are estimated bilaterally. (C) The temporal specificity of this correlation is revealed through movement aligned sample-wise correlations of average force predictions with UPDRS-III scores across patients (cluster based corrected significant segments are displayed shaded).

Spatial distribution of grip-force decoding performance in cortical and subthalamic recordings

The spatial distributions of decoding performance on cortex and STN for contra- and ipsilateral movements are shown in Figure 6. To evaluate the relevance of recording location with respect to decoding performance, we calculated correlations of performance measures with a priori defined implantation targets, dorsolateral STN(Caire et al., 2013; Horn et al., 2017a) and hand-knob of the precentral gyrus.(Mayka et al., 2006) Linear mixed effects models showed a significant within-subject relation for contralateral ECoG decoding performances (β=-0.002, Lower CI=-0.003, upper CI=-0.001, R^2= 0.57, p-value<0.001), but not STN locations (p > 0.05). The dependent variable was here the decoding performance, fixed effect the distance to hand knob area or dorsolateral STN respectively, and random effect the subject. Repeating the analysis across electrodes and patients in a cross-validated manner revealed no significant predictive value. Thus, Euclidean distance hand knob area for ECoG and therapeutic target for STN was significantly correlated with decoding performance within patients, but could not predict decoding performance across channels or patients.

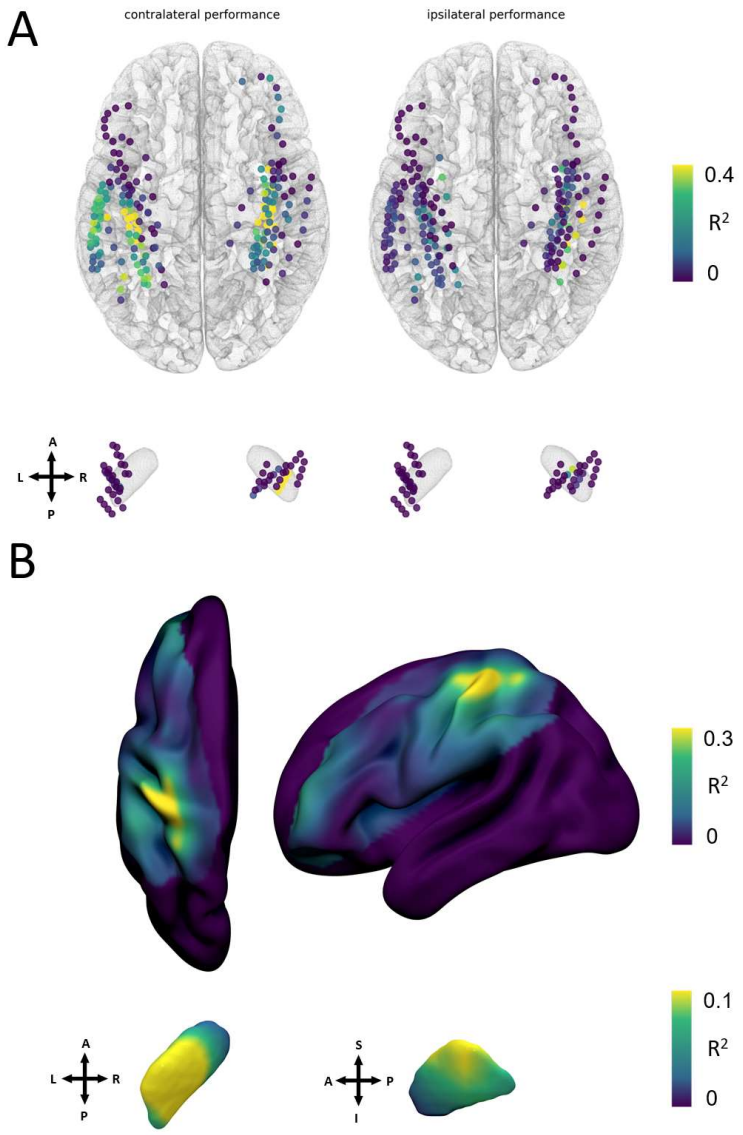

Figure 6: Mean test XGBOOST R^2 performances peak around cortical sensorimotor areas and the dorsolateral STN. (A) Channels are color coded for individual XGBOOST regression performances based on the best Bayesian Optimization hyperparameter set. Performance differences shown are in favor of ECoG over STN and contralateral over ipsilateral recording locations for movement decoding. (B) Interpolated cortex performance peaks in sensorimotor areas. STN interpolated decoding performance peaks at the dorsolateral STN which was shown to overlay with the optimal PD DBS target(Caire et al., 2013).

Whole brain connectomics can be used to cross-predict decoding performances across patients

The ability to account for decoding performances for invasive electrodes may soon become be as important as accounting for variance in therapeutic effects, as bidirectional clinical brain computer interfaces will rely

both on electrical sensing and stimulation. Recently, network mapping of neurostimulation effects has shown utility to predict variance in clinical outcomes following DBS.(Horn et al., 2017c; Horn and Fox, 2020; Li et al., 2020) Here, we extended the same framework to instead predict variance in grip-force decoding performance observed from single channels, using the XGBOOST grip-force decoding results. In this approach – termed *prediction network mapping* – we calculated functional and structural connectivity *fingerprints* by projecting each recording location to a group connectome that was acquired in a cohort of PD patients. These fingerprints denote to which other brain areas each site is connected to. Using a discriminative fiber tracking analysis,(Baldermann et al., 2019; Li et al., 2020) we analyzed the predictive value of structural connectivity from ECoG recording locations (for an exemplar case see Figure 7A) for XGBOOST decoding performance. Therefore, diffusion imaging derived whole-brain fiber connectome data traversing to more than 20% of recording locations (Figure 7B). The specific fiber distributions could significantly predict decoding performance of left out channels ($\rho = 0.38$, p-value < 0.0001; thresholded at false discovery rate $\alpha = 0.05$) and patients ($\rho = 0.37$, p-value < 0.0001) in a cross validated manner (Figure 7D).

Next, we created spatial models of optimal decoding performance for functional connectivity (R-Maps are shown in Figure 7C). This model led to significant predictions of decoding performance in leave-one-channel-out ($\rho = 0.37$, p-value < 0.0001) and leave-one-subject-out cross validations (functional connectivity $\rho = 0.37$, p-value < 0.0001) cross-validation (Figure 7E). Models such as the two presented here could be used to identify optimal networks that may be used to optimally decode behavior specific brain signals. The findings were further validated and confirmed using traditional voxel-wise statistical parametric mapping (see supplements).

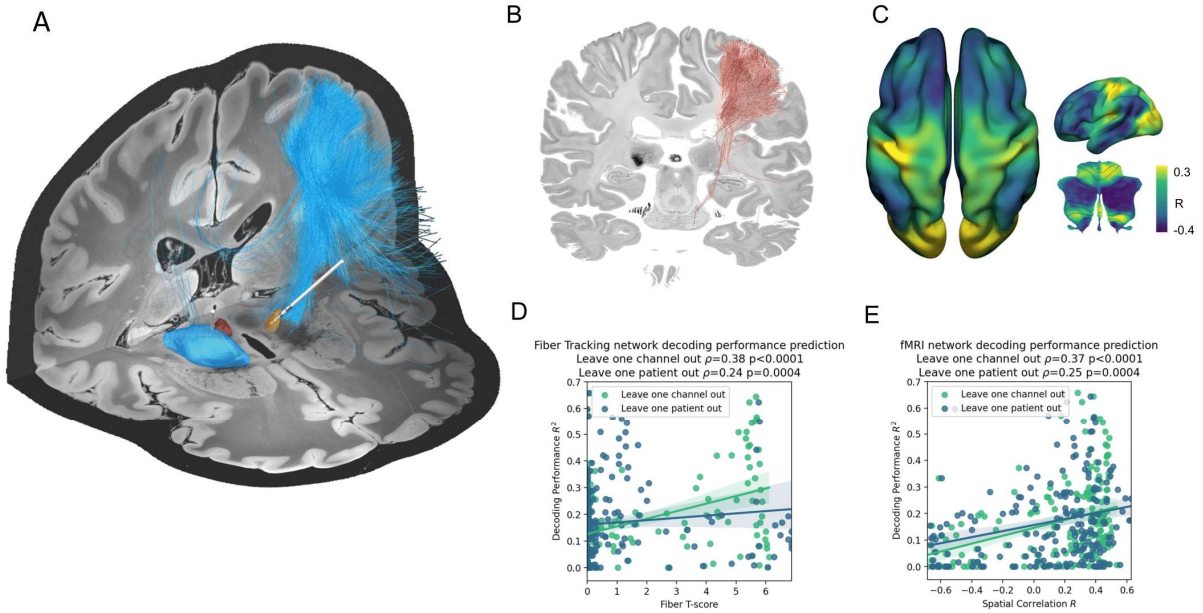

Figure 7: Structural and functional movement decoding network analysis reveals cerebellar as well as sensorimotor cortical decoding capacity. (A) Visualization of fibers originating from the ECoG recording locations of subject 1. (B) Decoding performance across all subjects and channels significant fiber tracts are displayed. All ECoG contacts were projected to the left hemisphere. For every fiber a t-test statistic between connected and unconnected brain regions was calculated. Only significant fibers, indicating structural connectivity to decoding performance, are shown. (C) The optimal R-Map is shown for the cortical surface as well as cerebellum for fMRI functional connectivity. Fingerprints were calculated between the functional connectivity of every electrode contact to all other voxels. The R-Map was then calculated as a correlation between individual contact fingerprints and the contact specific R^2 decoding performance. (D) Fiber tracking connectivity predicts decoding performance (leave one channel out cross validation ρ = 0.38, p < 0.0001, leave one patient out cross validation ρ = 0.24, p-value = 0.0004). Here each individual point represents a statistic of connected and unconnected fibers of each contact or patient. The previously calculated fiber statistic within each cross validation fold could thus predict the channel or patient specific performance. (E) Functional connectivity predicts decoding performance (leave one channel out cross validation ρ = 0.37, p < 0.0001, leave one patient out cross validation ρ = 0.25, p = 0.0004). The spatial correlation between individual fingerprints and the cross validation specific R-Map, predicts left out decoding performances.

Discussion

Bidirectional brain computer interfaces will revolutionize the treatment of previously intractable brain disorders with brain signal decoding based adaptive neuromodulation. DBS provides a unique platform to trailblaze neurophysiological approaches, disease specific modulation and computational strategies for next-generation brain implants improving PD symptoms. Here, we investigated clinical and computational strategies for grip-force decoding based on multimodal invasive neurophysiology in PD patients undergoing DBS neurosurgery. Our findings can be broken down into four advances to the field: 1) we developed a new decoding approach based on multispectral time-concatenated band-power measures, subjected to Bayesian optimized extreme gradient boosted ensembles (XGBOOST): this outperformed traditional linear

288 model-based methods and may be generalized to all brain signal-based regression problems. 2) Next, we
289 demonstrate that electrocorticography signals outperform subthalamic LFP for grip-force decoding,
290 supporting the utility of additional ECoG in adaptive DBS research for PD patients. 3) Our findings inversely
291 link PD motor impairment and decoding performance, highlighting a potential impairment in movement
292 coding capacity through PD pathophysiology. 4) Finally, we could significantly predict how well a specific
293 recording site would perform to decode grip force based on brain connectivity. This novel framework (termed
294 prediction network mapping) will be used in future implants to identify connectomic brain networks from
295 which brain sensing can predict symptoms and behavior.

296 *Limitations*

297 Our analysis is retrospective in nature. All model training and evaluations were conducted offline.
298 Nevertheless, we took meticulous care to exclude any circularity in processing and machine learning
299 applications. To this date, such circularities are overlooked in some movement decoding papers with
300 filtering, normalization and time frequency transformation across entire sessions, thus reaching into the
301 future from the point of the individually decoded sample. Ridding our analysis from data that would be
302 unavailable in a real-time setting as reported in this study, leads to worse performances, but gives a more
303 realistic estimate of model performance in the clinical use-case. An additional limitation was the relatively
304 small amount of available data, which was constrained by the intraoperative setting (see Table 1). For deep
305 learning approaches we hypothesize better performances with an increased dataset size, which in the future
306 will be obtained through longer term recordings, either with externalized leads(He et al., 2021) or sensing
307 enabled implantable devices.(Gilron et al., 2021; Opri et al., 2020)

308 *Decoding grip force based on invasive electrophysiology*

309 Our study defines a novel computational strategy to decode grip-force based on ECoG and LFP in patients
310 undergoing DBS for PD. It explores defined oscillatory feature sets and compares machine learning models
311 with varying complexity, from linear models to artificial neural networks and regression trees. ECoG based
312 movement decoding of varying movement types was previously reported in epilepsy patients that underwent
313 electrophysiological monitoring(Leuthardt et al., 2004) with local motor potential and gamma band activity
314 reported to be informative features.(Gunduz et al., 2016) Previous analyses on decoding of grip force based
315 on STN-LFPs was based on Wiener Filter architectures.(Shah et al., 2018; Tan et al., 2016) Here, our paper
316 extended previous reports to a continuous non-trial-based decoding approach. Furthermore, a direct
317 comparison of ECoG and LFP performance with relation to systematic machine learning methods was
318 lacking. Our findings indicate that sensorimotor ECoG recordings are more informative than LFP recordings
319 from the STN for grip-force decoding. Our results are based on extracted band-power features and show
320 superior performances with XGBOOST, when compared to other model architectures and algorithms. Best
321 performances were obtained by single channel ECoG recordings without additional benefit from channel
322 combinations or combined ECoG and STN channel sets. Single channel ECoG recordings combined with
323 XGBOOST shows significant potential for clinical real-time BCI in movement disorders(He et al., 2021; Opri
324 et al., 2020) and other motor system diseases such as stroke and spinal cord injury. Beyond movement

disorders, the proposed machine learning approach can be adopted to extend the clinical utility of invasive brain stimulation approaches for other brain disorders, e.g. through decoding of tics or obsessive compulsive behavior in neuropsychiatric DBS indications.

Towards machine learning based adaptive stimulation in Parkinson's disease

Adaptive and responsive neuromodulation has the potential for significant innovation in neuromodulation.(Starr, 2018) The beta single-(Arlotti et al., 2018; Little et al., 2013) or dual threshold(Velisar et al., 2019) based aDBS is now being investigated in clinical trials to improve the treatment for patients with akinetic rigid dominant PD (ClinicalTrials.gov Identifier: NCT04681534, NCT04547712). Beyond subthalamic beta, ECoG recordings were previously used to successfully indicate the presence of dyskinesia through elevated levels of gamma band synchronization and reduced stimulation intensity.(Swann et al., 2018) Single biomarker approaches have the advantage that pathophysiological mechanisms may be the direct target of intervention, while machine learning based decoding methods derive correlates of symptoms and behavior indirectly through learning potentially noisy correlations.(Neumann et al., 2019) Therefore, single biomarker aDBS presents an optimal starting point for investigating the clinical utility of aDBS in controlled study designs. However, single biomarkers alone cannot account for the diverse and complex set of clinical signs of PD and behavior, e.g. during gait,(Molina et al., 2021) speech and tremor.(Hirschmann et al., 2017, 2013) Here a versatile decoding based control algorithm may further improve clinical outcome for these patients in future.(Neumann et al., 2019) Indeed, machine learning-based decoding has been successfully described in first translational breakthrough studies.(Gilron et al., 2021; He et al., 2021; Opri et al., 2020) In a complementary approach, we focused on direct grip-force decoding, motivated by the hypothesis that future aDBS studies increasing DBS amplitude during periods of higher movement vigor may advance the successful treatment of bradykinesia in PD. While studies indicate that relative amounts of beta can still signal bradykinesia during movement,(Feldmann et al., 2021; Lofredi et al., 2019) further positive control parameters could keep stimulation proportional to movement vigor. Moreover, recent reports that beta power correlates negatively with phasic dopamine release may further motivate the idea of movement/kinematics based STN stimulation to support intrinsic movement related dopamine signals.(Schwerdt et al., 2020) To elaborate, given that DBS suppresses local firing of the subthalamic nucleus,(Milosevic et al., 2018) this may constitute a network modulation on the indirect pathway that is similar to the effect dopamine. In a recent non-human primate study it was shown that phasic decreases in beta in the basal ganglia are correlated to phasic dopamine signals during movement.(Schwerdt et al., 2020) Thus, in order to support the intrinsic dopaminergic capacity of PD patients, future machine learning based aDBS approaches could be complemented by algorithms that inform the stimulation on behavioral and motor adjustments to mimic intrinsic phasic dopamine signals. Previous studies have successfully decoded the presence of movement using cortical beta activity,(Opri et al., 2020) which may also be viable in PD. However, getting an estimate of movement vigor i.e. through the prediction of grip-force may complement advanced aDBS control policies, as multivariate models emerge for the next-generation of neurotherapeutics.

362 Beyond direct aDBS control, machine learning based brain signal decoding may also have diagnostic utility
363 for monitoring motor symptom severity and could inform additional control algorithms to account for bias in
364 traditional biomarkers such as beta and gamma elicited through other voluntary actions.(Neumann et al.,
365 2019) Importantly, we demonstrate that motor symptom severity itself can have direct negative effects on
366 decoding performance, which we should keep in mind during clinical decision making. Previously on a single
367 trial level, the presence of beta bursts correlated with motor performance in cortex(Little et al., 2019) and
368 STN,(Torrecillos et al., 2018) which could degrade decoding performance.(Khawaldeh et al., 2020) Our
369 findings indicate general impact of motor symptoms in the hypodopaminergic state on machine learning
370 based kinematic decoding capacity. This finding highlights the conceptual relevance of disease specific
371 interactions with computational models. Interestingly, in the hypodopaminergic state, the model output
372 underestimated the grip force extent produced by the patients. It may be speculated that this reflects a loss
373 of neural vigor representations related to insufficient dopaminergic modulation.(Turner and Desmurget,
374 2010) In the future, we will have to account for the individual impact of disease specific changes in brain
375 signals that affect decoding performance. Further, our results corroborate the notion that dopamine plays a
376 key role in coding and modulating neural representations of movement kinematics in the human brain.

377 *Brain connectivity can help identifying networks with high decoding performance*

378 Decoding performance for clinical BCI may be drastically improved when adjusting brain signal recording
379 sites to the underlying interconnected network that is relevant to the specific behavior that is being decoded.
380 For instance, when decoding language or speech, one could picture that recordings at either Broca's or
381 Wernicke's region could be helpful, but a combination of both could be better. The two regions form a
382 network with direct connections via the Arcuate Fascicle. Based on the data we have, which spans across
383 multiple brain regions across the entire cohort, we aimed at identifying the network that would be most useful
384 to decode grip force. For this endeavor, we adapted two existing methods that are able to isolate i)
385 connected voxels and ii) connected fibertracts methods(Horn et al., 2017c; Li et al., 2020) associated with
386 a specific effect (such as decoding performance in the present case). While Euclidean distance to motor
387 target, i.e. hand knob area for ECoG and therapeutic target for STN, was significantly correlated with
388 decoding performance within-subject, this simplistic notion could not predict decoding performance across
389 channels or patients. Thus, proximity to landmarks alone does not reliably help the identification of optimal
390 recording sites. Given the complexity and vast distribution of movement related brain areas, from cerebellum
391 to frontal cortex to parietal cortex, it may not be surprising that whole brain connectomics outperform single
392 ROI based distance metrics for predicting informative recording locations. Commonly BCI performance is
393 highly dependent on single subject training. Using optimal decoding performance whole-brain connectivity
394 can in turn significantly boost decoding performance across patients, possibly even without patient individual
395 training. Such connectomic models can be trained based on multiple dimensions of input-output
396 relationships, e.g. decoding of behavior like grip-force, but also clinical signs, such as tremor. For psychiatric
397 disorders such as obsessive-compulsive disorder or treatment resistant depression, this approach can be
398 used to target specific networks related to target symptoms. Thus, our results highlight the utility of whole-

399 brain connectomics to predict machine learning-based brain signal decoding performance that can be
400 generalized to any bidirectional clinical brain-computer interface use case. In the future, neurosurgeons may
401 not target individual locations in isolation, but instead determine optimal implant trajectories in accordance
402 with whole-brain connectomic fingerprints for optimal BCI performance.

403 *Conclusion*

404 Our analysis from PD patients undergoing DBS implantation showed that ECoG recordings outperform STN-
405 LFP recordings for grip-force decoding throughout different machine learning methods, with XGBOOST
406 showing the highest performance. Parkinsonian motor symptom severity was associated with loss of
407 decoding performance, indicating a specific link of kinematic coding capacity and motor impairment. Next,
408 we have formalized a connectomic framework that could cross-predict decoding performances across
409 recording sites and patients, based on underlying whole brain MRI connectivity patterns. Our findings
410 highlight the utility of ECoG for intelligent adaptive stimulation in PD, corroborate the role of PD symptom
411 severity in kinematic coding and pave the way for connectomic neurosurgery for machine learning-based
412 brain signal decoding. We hypothesize that future neurotechnological treatments may have the potential to
413 outperform traditional drug regimes, due to a key advantage in the temporal (and spatial) precision of
414 therapeutic delivery. Treatment can be aligned to changes of therapeutic demand, paving the way for a
415 precision medicine approach toward individualized symptom-specific DBS.(He et al., 2021; Neumann and
416 Rodriguez-Oroz, 2021; Neumann et al., 2019; Opri et al., 2020)

417 **Materials and Methods**

418 *Participants*

419 The current study is based on previously published data.(Alhourani et al., 2020) In brief, subthalamic LFP
420 and subdural ECoG recordings were simultaneously acquired from 11 PD patients. The patients were
421 subjected to bilateral STN DBS lead implantation, as proposed by standard clinical indications criteria. In
422 accordance with protocol #PRO13110420, approved by the Institutional Review Board of the University of
423 Pittsburgh, informed consent for all patients was obtained prior to any surgical procedure. The subject
424 characteristics are detailed in Table 1. UPDRS Part III scores for the off-medication conditions were
425 collected in a time period of 1-3 months prior to surgery by movement disorder neurologists.
426 Antiparkinsonian medications were held for at least 12 hours before intraoperative testing.

427

428 Table 1: Subject characteristics

N	Gender	UPDRS total	Hemisphere	Age	Movements	Disease duration [years]	ECoG Strip Contact Number Left	ECoG Strip Contact Number Right
0	Male	28	R	60.3	128	10.7	0	6
1	Male	27	L+R	51.2	464	14	28	28
2	Male	33	L+R	53.8	213	7.2	8	8
3	Male	31	L+R	44.2	285	10.1	8	8
4	Male	32	2L+2R	63.6	381	13.1	28+8	28+8
5	Male	52	L	59.6	84	5.9	6	0
6	Male	55	L	71.6	161	1.4	6	0
7	Male	50	L	52.5	131	8.7	6	0
8	Male	62	L+R	66.8	547	9.8	6	6
9	Male	48	L	67.9	86	17.1	6	0
10	Female	31	R	69	205	10.4	0	6

429

430 *Behavioral Paradigm*

431 The behavioral task performed for this study was previously described(Alhourani et al., 2020; Fischer et al.,
432 2020; Kondylis et al., 2016) and it is schematically shown in Figure 1A. Subjects were fully awake, and no
433 anesthetic agents were administered for at least 1 hour before the task procedure. No medication was given
434 during the task.

435 The task paradigm was implemented using the Psychophysics Toolbox(Brainard, 1997) on a portable
436 computer. The trials consisted of a simultaneous presentation of a yellow traffic light in the center of a
437 screen, and a cue on one side indicating which hand the subject should use for the subsequent response
438 of squeezing the handgrip. The cue remained on screen for 1000-2000 ms, followed by the traffic light
439 changing either green or red, signaling a ‘’go cue’’ and ‘’no-go cue’’ respectively. Subjects performed the
440 task for a cumulative total time of 10 to 25 min. As the present study focuses on grip-force decoding
441 performance based on the electrophysiological signals, all sessions containing valid movements were
442 merged per subject for further analysis. To validate that the used grip-force label in our data varies not only
443 between two movement states, but constitutes a relevant regression problem with varying force amplitude
444 and velocity, all movement maximum amplitudes and velocity traces are visualized in the Supplementary
445 Figure 1.

446 *Electrophysiological Recordings*

447 ECoG data were recorded intra-operatively from subjects with PD using six-contact (left n = 5 patients, right
448 n = 3), eight-contact (left n = 3, right n = 3) and twenty-eight-contact (left n = 2, right n = 2) strip electrodes.
449 The electrode details are shown in Supplementary Table 1 and all ECoG and STN electrodes are plotted in
450 Figure 1B (mean number of electrode contacts were 10.18±11.29 for left and 8.9±12 for right hemispheres).
451 A referential montage was used in which the reference electrode was placed in the scalp and a ground
452 electrode was placed in the skin overlying the acromion process. The used electrode localization procedure
453 was described in detail earlier.(Randazzo et al., 2016) In brief, preoperative MRI and postoperative CT
454 scans were co-registered and normalized to MNI 2009b NLIN ASYM space. Electrode artefacts were
455 visually identified and marked to obtain MNI coordinates of DBS electrode contacts (see supplementary
456 materials for more details). LFP data from the lead were obtained after clinical stimulation testing was
457 completed. ECoG and STN signals were filtered (0.3–7.5 kHz), amplified, and digitized at 30 kHz using a
458 Grapevine neural interface processor (Ripple Inc.). Force signals were digitally recorded simultaneously
459 with the ECoG and STN-LFP signals. LFPs from the STN were recorded using the clinical DBS lead (model
460 3389, Medtronic) from all four contacts and referenced offline in a bipolar montage. All signals were
461 resampled to 1 kHz for offline analysis.

462 *ECoG and LFP preprocessing and feature extraction*

463 The entire preprocessing pipeline used in the present study was optimized for real-time performance and
464 inspired by the Berlin Brain Computer Interface.(Blankertz et al., 2006) Processing was performed in Python
465 using custom code based on MNE-python,(Gramfort et al., 2013) mne_bids (Appelhoff et al., 2019) and
466 pybv (https://pybv.readthedocs.io/en/stable/). All raw data files were saved in the iEEG-BIDS
467 structure.(Holdgraf et al., 2019) To account for baseline drifts, the force traces were cleaned using a
468 normalization approach presented for previous ECoG finger trajectory decoding.(Xie et al., 2018) A real-
469 time data stream of untouched electrophysiological raw data was emulated to ensure that all processing
470 that can impact decoding is performed in a real-time compatible manner. Referencing was performed online,
471 where all LFP recordings were referenced bipolarly, against the adjacent contacts (0-1, 1-2, 2-3 with contact
472 0 being the lowest by convention of the manufacturer). ECoG recordings were referenced by subtracting
473 the common average of all ECoG electrodes. To adhere to most computationally efficient real-time enabled
474 algorithms, time frequency decomposition for the machine learning analysis was conducted by bandpass
475 filtering in the θ (4-8 Hz), α (8-12 Hz), β (13-35 Hz), low β (13-20 Hz), high β (20-35 Hz), all γ (60-200 Hz),
476 γ (60-80 Hz) and high-frequency activity, (90-200 Hz) frequency bands. Overlapping broad β and γ bands
477 were added in addition to subbands to enable the investigation of distinct interactions within these frequency
478 bands (Figure 1C). To estimate band specific activity, different time durations were used for band pass
479 filtering with longer time segments for lower frequencies, and shorter time segments for higher frequencies
480 (θ = 1000 ms, α and β bands = 500 ms, γ = 100 ms). To get an estimate of amplitude of the activity in the
481 filtered signals, variance was extracted in intervals of 1 s in a sliding window of 100 ms resulting in a time
482 resolution of 10 Hz. All variance estimates were normalized by subtracting and dividing by the median in a

483 sliding window of 10 s to account for differences in impedance and proximity to the source before subjecting
484 the data to the machine learning analysis. By a fixed parameter of -2 and 2 after normalization, all features
485 were clipped as an artifact rejection mechanism. The used normalization is based on the real time prediction
486 approach, such that data acquired in the future do not influence the present predictions. See figure 1E for
487 an outline of the methods pipeline. For the purpose of visualization, Morlet wavelets (7 cycles) were used
488 to demonstrate the entire time-frequency decomposition (Figure 1C).

489 *Machine learning training and evaluation*

490 A rigorous nested cross validation approach was implemented. An outer 3-fold cross validation split the data
491 into folds of two third training and one third test set non shuffled. For each individual channel a Bayesian
492 Optimization hyperparameter search(Frazier, 2018) was then conducted for at least 10 rounds using the
493 training set only. For each round the training data was trained and tested in an inner non shuffled 3-fold
494 cross-validation with 80 percent training size. The mean R^2 coefficient of determination of every test set
495 estimate of the outer cross-validation was used as the performance measure. R^2 values were Fisher-
496 transformed through the inverse hyperbolic tangent function to approximate a normal distribution for further
497 statistics.(Fisher, 1915) The input features for every model were all eight previously described frequency
498 bands. In order to test the contribution of previous time points, frequency band features of different time
499 points were concatenated and compared according to their decoding performance. The present study
500 investigated commonly used and promising linear and non-linear machine learning algorithms, specifically
501 elastic net regularized linear models, linear Wiener filters, neural networks, gradient boosted decision trees
502 (XGBOOST) and source power comodulation were trained to decode grip-force traces. All models
503 underwent an extensive hyperparameter search using Bayesian optimization. The motivation behind the
504 used methods as well as the respective hyperparameter search spaces are explained in detail in the
505 supplementary materials. The chosen methodology is non-exhaustive and primarily serves the comparison
506 of variance in decoding explained by the recording location of the signal (ECoG vs. STN) and motor
507 symptom severity (UPDRS-III). It further gives an intuition about the potential of more complex and elaborate
508 machine learning methods for brain computer interfaces.

509 *Definition of best model and best channels*

510 Previous studies have repeatedly demonstrated that using a single optimal channel in the STN is
511 advantageous over using all available channels.(Shah et al., 2018) Most importantly, addition of more
512 channels leads to decreased generalization and higher risk of overfitting with little performance benefit.
513 Based on these results and to account for varying numbers of available electrode contacts, one channel
514 with optimal decoding performance on the cross-validation test set was chosen per patient to quantify and
515 compare decoding performance for the ECoG and STN analysis across patients. Since hyperparameter
516 optimization is implemented only within each inner cross validation fold, any circularity and data leakage is
517 circumvented. A robust decoding performance estimate is thus obtained through left out testing data only.

Prediction Network Mapping with whole-brain connectomics

To investigate whether decoding performance from different recording locations can cross-predict across patients, we developed a whole-brain connectomics based approach. Therefore, ECoG electrode recording locations were projected to normative structural and functional MRI data (Parkinson's Progression Markers Initiative [PPMI]; www.ppmi-info.org) using Lead-DBS software in Matlab (www.lead-dbs.org).(Horn et al., 2019) The PPMI connectomes of patients with PD (n = 74) was priorly computed(Ewert et al., 2018) and has been used in context of DBS multiple times.(de Almeida Marcelino et al., 2019; Horn et al., 2017b; Lofredi et al., 2021; Neumann et al., 2018) Seeding from each recording site resulted in connectivity profiles (fingerprints) that were expressed as voxel-wise whole-brain volumes for functional and structural connectivity and a set of streamline connections for structural connectivity. We have adapted three previously published methods leveraging normative connectomes as predictive models.

First, fiber streamlines representative of structural connectivity between ECoG channels and all other brain areas were isolated and assigned with a "Fiber T-score", associating XGBOOST decoding performance with the fiber tracts connectivity from respective ECoG recording locations across patients using mass-univariate two-sample t-tests between R^2 scores in connected vs. unconnected recording locations. Only fibers with significant t-scores surviving FDR correction at an alpha level 0.05 were considered further. Next, T-values were used as weights in an aggregated fiber score to predict out of training sample channel and patients' performances. Next, functional connectivity maps were used to generate an "R-Map", a connectivity model which is associated with optimal decoding performance, by performing voxel-wise correlations of connectivity and decoding performance from recording locations. The spatial fingerprint from each recording location can then be assigned a spatial correlation coefficient that may have predictive value for the underlying decoding performance. The predictive value of these two methods were confirmed using "leave-one-channel-out" and "leave-one-subject-out" cross-validation. Finally, statistical parametric mapping was used to confirm the described correlations of structural and functional connectivity using linear-mixed effects models (see supplementary results). All connectivity analyses were performed using ECoG recording locations with contralateral R^2 performances (Figure 1E).

Statistical Analysis

Results are stated as mean ± standard deviation. All significance testing was performed using two-sided Monte-Carlo permutation testing and bootstrapping. P-values were obtained by shuffling value positions and determining the resulting original rho value percentile in the distribution of surrogate combinations. Clinical correlations were performed between decoding performances and UPDRS-III total scores. To test for the temporal specificity of the clinical correlation, we performed sample-wise correlations of decoding output with UPDRS-III total scores across subjects. Multiple comparisons were corrected by adjusting the significance threshold α to the false discovery rate.(Benjamini and Hochberg, 2000)

Data availability

All used data will be made available upon request. The code for the reproduction of every Figure, machine learning and statistical analysis are openly available at the GitHub repository (https://github.com/neuromodulation/icn/tree/master/ECOG_vs_STN).

Funding

The present manuscript was supported through a US-German Collaborative Research in Computational Neuroscience (CRCNS) grant to R.S.T., R.M.R. and W.J.N. with funding from the German Federal Ministry for Research and Education and NIH (R01NS110424). Further funding was provided through Deutsche Forschungsgemeinschaft (DFG, German Research Foundation) – Project-ID 424778371 – TRR 295 to A.H. and W.J.N.

A.H. was supported by the German Research Foundation (Deutsche Forschungsgemeinschaft, Emmy Noether Stipend 410169619 and 424778371 – TRR 295) as well as Deutsches Zentrum für Luft- und Raumfahrt (DynaSti grant within the EU Joint Programme Neurodegenerative Disease Research, JPND).

Some data used in the preparation of this article were obtained from the PPMI database (www.ppmi-info.org/data). For up-to-date information on the study, visit www.ppmi-info.org. PPMI, a public–private partnership, is funded by the Michael J. Fox Foundation for Parkinson's Research. For funding partners, see www.ppmi-info.org/fundingpartners.

References

Alhourani A, Korzeniewska A, Wozny TA, Lipski WJ, Kondylis ED, Ghuman AS, Crone NE, Crammond DJ, Turner RS, Richardson RM. 2020. Subthalamic Nucleus Activity Influences Sensory and Motor Cortex during Force Transduction. *Cerebral Cortex* **30**:2615–2626. doi:10.1093/cercor/bhz264

Androulidakis AG, Kuhn AA, Chu Chen C, Blomstedt P, Kempf F, Kupsch A, Schneider G-H, Doyle L, Dowsey-Limousin P, Hariz MI, Brown P. 2007. Dopaminergic therapy promotes lateralized motor activity in the subthalamic area in Parkinson's disease. *Brain* **130**:457–468. doi:10.1093/brain/awl358

Appelhoff S, Sanderson M, Brooks TL, Vliet M van, Quentin R, Holdgraf C, Chaumon M, Mikulan E, Tavabi K, Höchenberger R, Welke D, Brunner C, Rockhill AP, Larson E, Gramfort A, Jas M. 2019. MNE-BIDS: Organizing electrophysiological data into the BIDS format and facilitating their analysis. *Journal of Open Source Software* **4**:1896. doi:10.21105/joss.01896

Arlotti M, Marceglia S, Foffani G, Volkmann J, Lozano AM, Moro E, Cogiamanian F, Prenassi M, Bocci T, Cortese F, Rampini P, Barbieri S, Priori A. 2018. Eight-hours adaptive deep brain stimulation in patients with Parkinson disease. *Neurology* **90**:e971–e976. doi:10.1212/WNL.0000000000005121

Baldermann JC, Melzer C, Zapf A, Kohl S, Timmermann L, Tittgemeyer M, Huys D, Visser-Vandewalle V, Kühn AA, Horn A, Kuhn J. 2019. Connectivity Profile Predictive of Effective Deep Brain Stimulation in Obsessive-Compulsive Disorder. *Biological Psychiatry*, Neurodevelopmental Mechanisms of Obsessive-Compulsive Disorder and Autism **85**:735–743. doi:10.1016/j.biopsych.2018.12.019

Benjamini Y, Hochberg Y. 2000. On the Adaptive Control of the False Discovery Rate in Multiple Testing With Independent Statistics. *Journal of Educational and Behavioral Statistics* **25**:60–83. doi:10.3102/10769986025001060

Beudel M, Brown P. 2016. Adaptive deep brain stimulation in Parkinson's disease. *Parkinsonism Relat Disord* **22 Suppl 1**:S123-126. doi:10.1016/j.parkreldis.2015.09.028

Blankertz B, Dornhege G, Lemm S, Krauledat M, Curio G, Müller K-R. 2006. The Berlin Brain-Computer Interface: Machine Learning Based Detection of User Specific Brain States. *Journal of Universal Computer Science* **12**:581Â 607.

Brainard DH. 1997. The Psychophysics Toolbox. *Spatial Vision* **10**:433–436. doi:10.1163/156856897X00357

Cagnan H, Denison T, McIntyre C, Brown P. 2019. Emerging technologies for improved deep brain stimulation. *Nature Biotechnology* **37**:1024–1033. doi:10.1038/s41587-019-0244-6

Caire F, Ranoux D, Guehl D, Burbaud P, Cuny E. 2013. A systematic review of studies on anatomical position of electrode contacts used for chronic subthalamic stimulation in Parkinson's disease. *Acta Neurochir (Wien)* **155**:1647–1654; discussion 1654. doi:10.1007/s00701-013-1782-1

Chen T, Guestrin C. 2016. XGBoost: A Scalable Tree Boosting SystemProceedings of the 22nd ACM SIGKDD International Conference on Knowledge Discovery and Data Mining, KDD '16. New York, NY, USA: Association for Computing Machinery. pp. 785–794. doi:10.1145/2939672.2939785

Cole SR, van der Meij R, Peterson EJ, de Hemptinne C, Starr PA, Voytek B. 2017. Nonsinusoidal Beta Oscillations Reflect Cortical Pathophysiology in Parkinson's Disease. *J Neurosci* **37**:4830–4840. doi:10.1523/JNEUROSCI.2208-16.2017

Dähne S, Meinecke FC, Haufe S, Höhne J, Tangermann M, Müller K-R, Nikulin VV. 2014. SPoC: a novel framework for relating the amplitude of neuronal oscillations to behaviorally relevant parameters. *Neuroimage* **86**:111–122. doi:10.1016/j.neuroimage.2013.07.079

de Almeida Marcelino AL, Horn A, Krause P, Kühn AA, Neumann W-J. 2019. Subthalamic neuromodulation improves short-term motor learning in Parkinson's disease. *Brain* **142**:2198–2206. doi:10.1093/brain/awz152

de Hemptinne C, Swann NC, Ostrem JL, Ryapolova-Webb ES, San Luciano M, Galifianakis NB, Starr PA. 2015. Therapeutic deep brain stimulation reduces cortical phase-amplitude coupling in Parkinson's disease. *Nat Neurosci* **18**:779–786. doi:10.1038/nn.3997

Ewert S, Plettig P, Li N, Chakravarty MM, Collins DL, Herrington TM, Kühn AA, Horn A. 2018. Toward defining deep brain stimulation targets in MNI space: A subcortical atlas based on multimodal MRI, histology and structural connectivity. *Neuroimage* **170**:271–282. doi:10.1016/j.neuroimage.2017.05.015

Feldmann LK, Neumann W-J, Krause P, Lofredi R, Schneider G-H, Kühn AA. 2021. Subthalamic beta band suppression reflects effective neuromodulation in chronic recordings. *Eur J Neurol* **28**:2372–2377. doi:10.1111/ene.14801

Fischer P, Lipski WJ, Neumann W-J, Turner RS, Fries P, Brown P, Richardson RM. 2020. Movement-related coupling of human subthalamic nucleus spikes to cortical gamma. *eLife* **9**:e51956. doi:10.7554/eLife.51956

Fisher RA. 1915. Frequency Distribution of the Values of the Correlation Coefficient in Samples from an Indefinitely Large Population. *Biometrika* **10**:507–521. doi:10.2307/2331838

Frazier PI. 2018. A Tutorial on Bayesian Optimization. *arXiv preprint arXiv:10122599*.

Gilron R, Little S, Perrone R, Wilt R, de Hemptinne C, Yaroshinsky MS, Racine CA, Wang SS, Ostrem JL, Larson PS, Wang DD, Galifianakis NB, Bledsoe IO, San Luciano M, Dawes HE, Worrell GA, Kremen V, Borton DA, Denison T, Starr PA. 2021. Long-term wireless streaming of neural recordings for circuit discovery and adaptive stimulation in individuals with Parkinson's disease. *Nat Biotechnol* 1–8. doi:10.1038/s41587-021-00897-5

Gramfort A, Luessi M, Larson E, Engemann DA, Strohmeier D, Brodbeck C, Goj R, Jas M, Brooks T, Parkkonen L, Hämäläinen M. 2013. MEG and EEG data analysis with MNE-Python. *Front Neurosci* **7**. doi:10.3389/fnins.2013.00267

Gunduz A, Brunner P, Sharma M, Leuthardt EC, Ritaccio AL, Pesaran B, Schalk G. 2016. Differential roles of high gamma and local motor potentials for movement preparation and execution. *Brain-Computer Interfaces* **3**:88–102. doi:10.1080/2326263X.2016.1179087

He S, Baig F, Mostofi A, Pogosyan A, Debarros J, Green AL, Aziz TZ, Pereira E, Brown P, Tan H. 2021. Closed-Loop Deep Brain Stimulation for Essential Tremor Based on Thalamic Local Field Potentials. *Movement Disorders* **36**:863–873. doi:10.1002/mds.28513

Hirschmann J, Hartmann CJ, Butz M, Hoogenboom N, Özkurt TE, Elben S, Vesper J, Wojtecki L, Schnitzler A. 2013. A direct relationship between oscillatory subthalamic nucleus–cortex coupling and rest tremor in Parkinson's disease. *Brain* **136**:3659–3670. doi:10.1093/brain/awt271

Hirschmann J, Schoffelen JM, Schnitzler A, van Gerven MAJ. 2017. Parkinsonian rest tremor can be detected accurately based on neuronal oscillations recorded from the subthalamic nucleus. *Clinical Neurophysiology* **128**:2029–2036. doi:10.1016/j.clinph.2017.07.419

Holdgraf C, Appelhoff S, Bickel S, Bouchard K, D'Ambrosio S, David O, Devinsky O, Dichter B, Flinker A, Foster BL, Gorgolewski KJ, Groen I, Groppe D, Gunduz A, Hamilton L, Honey CJ, Jas M, Knight R, Lachaux J-P, Lau JC, Lee-Messer C, Lundstrom BN, Miller KJ, Ojemann JG, Oostenveld R, Petridou N, Piantoni G, Pigorini A, Pouratian N, Ramsey NF, Stolk A, Swann NC, Tadel F, Voytek B, Wandell BA, Winawer J, Whitaker K, Zehl L, Hermes D. 2019. iEEG-BIDS, extending the Brain Imaging Data Structure specification to human intracranial electrophysiology. *Sci Data* **6**:102. doi:10.1038/s41597-019-0105-7

Horn A, Fox MD. 2020. Opportunities of connectomic neuromodulation. *NeuroImage* **221**:117180. doi:10.1016/j.neuroimage.2020.117180

Horn A, Kühn AA, Merkl A, Shih L, Alterman R, Fox M. 2017a. Probabilistic conversion of neurosurgical DBS electrode coordinates into MNI space. *NeuroImage* **150**:395–404. doi:10.1016/j.neuroimage.2017.02.004

Horn A, Li N, Dembek TA, Kappel A, Boulay C, Ewert S, Tietze A, Husch A, Perera T, Neumann W-J, Reisert M, Si H, Oostenveld R, Rorden C, Yeh F-C, Fang Q, Herrington TM, Vorwerk J, Kühn AA. 2019. Lead-DBS v2: Towards a comprehensive pipeline for deep brain stimulation imaging. *NeuroImage* **184**:293–316. doi:10.1016/j.neuroimage.2018.08.068

Horn A, Neumann W-J, Degen K, Schneider G-H, Kühn AA. 2017b. Toward an electrophysiological "sweet spot" for deep brain stimulation in the subthalamic nucleus. *Hum Brain Mapp* **38**:3377–3390. doi:10.1002/hbm.23594

Horn A, Reich M, Vorwerk J, Li N, Wenzel G, Fang Q, Schmitz-Hübsch T, Nickl R, Kupsch A, Volkmann J, Kühn AA, Fox MD. 2017c. Connectivity Predicts deep brain stimulation outcome in Parkinson disease. *Ann Neurol* **82**:67–78. doi:10.1002/ana.24974

Hwang BY, Salimpour Y, Tsehay YK, Anderson WS, Mills KA. 2020. Perspective: Phase Amplitude Coupling-Based Phase-Dependent Neuromodulation in Parkinson's Disease. *Front Neurosci* **14**:558967. doi:10.3389/fnins.2020.558967

Kehnemouyi YM, Wilkins KB, Anidi CM, Anderson RW, Afzal MF, Bronte-Stewart HM. 2021. Modulation of beta bursts in subthalamic sensorimotor circuits predicts improvement in bradykinesia. *Brain* **144**:473–486. doi:10.1093/brain/awaa394

Khawaldeh S, Tinkhauser G, Shah SA, Peterman K, Debove I, Khoa Nguyen TA, Nowacki A, Lenard Lachenmayer M, Schuepbach M, Pollo C, Krack P, Woolrich M, Brown P. 2020. Subthalamic nucleus activity dynamics and limb movement prediction in Parkinson's disease. *Brain* **143**:582–586. doi:10.1093/brain/awz417

Kondylis ED, Randazzo MJ, Alhourani A, Lipski WJ, Wozny TA, Pandya Y, Ghuman AS, Turner RS, Crammond DJ, Richardson RM. 2016. Movement-related dynamics of cortical oscillations in Parkinson's disease and essential tremor. *Brain* **139**:2211–2223. doi:10.1093/brain/aww144

Krauss JK, Lipsman N, Aziz T, Boutet A, Brown P, Chang JW, Davidson B, Grill WM, Hariz MI, Horn A, Schulder M, Mammis A, Tass PA, Volkmann J, Lozano AM. 2021. Technology of deep brain stimulation: current status and future directions. *Nat Rev Neurol* **17**:75–87. doi:10.1038/s41582-020-00426-z

Kühn AA, Kupsch A, Schneider G-H, Brown P. 2006. Reduction in subthalamic 8-35 Hz oscillatory activity correlates with clinical improvement in Parkinson's disease. *Eur J Neurosci* **23**:1956–1960. doi:10.1111/j.1460-9568.2006.04717.x

Kühn AA, Williams D, Kupsch A, Limousin P, Hariz M, Schneider GH, Yarrow K, Brown P. 2004. Event-related beta desynchronization in human subthalamic nucleus correlates with motor performance. *Brain* **127**:735–746. doi:10.1093/brain/awh106

Leuthardt EC, Schalk G, Wolpaw JR, Ojemann JG, Moran DW. 2004. A brain-computer interface using electrocorticographic signals in humans. *J Neural Eng* **1**:63–71. doi:10.1088/1741-2560/1/2/001

Li N, Baldermann JC, Kibleur A, Treu S, Akram H, Elias GJB, Boutet A, Lozano AM, Al-Fatly B, Strange B, Barcia JA, Zrinzo L, Joyce E, Chabardes S, Visser-Vandewalle V, Polosan M, Kuhn J, Kühn AA, Horn A. 2020. A unified connectomic target for deep brain stimulation in obsessive-compulsive disorder. *Nat Commun* **11**:3364. doi:10.1038/s41467-020-16734-3

Little S, Bonaiuto J, Barnes G, Bestmann S. 2019. Human motor cortical beta bursts relate to movement planning and response errors. *PLOS Biology* **17**:e3000479. doi:10.1371/journal.pbio.3000479

Little S, Pogosyan A, Neal S, Zavala B, Zrinzo L, Hariz M, Foltynie T, Limousin P, Ashkan K, FitzGerald J, Green AL, Aziz TZ, Brown P. 2013. Adaptive deep brain stimulation in advanced Parkinson disease. *Annals of Neurology* **74**:449–457. doi:10.1002/ana.23951

Lofredi R, Auernig GC, Irmen F, Nieweler J, Neumann W-J, Horn A, Schneider G-H, Kühn AA. 2021. Subthalamic stimulation impairs stopping of ongoing movements. *Brain* **144**:44–52. doi:10.1093/brain/awaa341

Lofredi R, Neumann W-J, Bock A, Horn A, Huebl J, Siegert S, Schneider G-H, Krauss JK, Kühn AA. 2018. Dopamine-dependent scaling of subthalamic gamma bursts with movement velocity in patients with Parkinson's disease. *eLife* **7**. doi:10.7554/eLife.31895

Lofredi R, Tan H, Neumann W-J, Yeh C-H, Schneider G-H, Kühn AA, Brown P. 2019. Beta bursts during continuous movements accompany the velocity decrement in Parkinson's disease patients. *Neurobiol Dis* **127**:462–471. doi:10.1016/j.nbd.2019.03.013

Mayka MA, Corcos DM, Leurgans SE, Vaillancourt DE. 2006. Three-dimensional locations and boundaries of motor and premotor cortices as defined by functional brain imaging: a meta-analysis. *Neuroimage* **31**:1453–1474. doi:10.1016/j.neuroimage.2006.02.004

Milosevic L, Kalia SK, Hodaie M, Lozano AM, Fasano A, Popovic MR, Hutchison WD. 2018. Neuronal inhibition and synaptic plasticity of basal ganglia neurons in Parkinson's disease. *Brain* **141**:177–190. doi:10.1093/brain/awx296

Molina R, Hass CJ, Cernera S, Sowalsky K, Schmitt AC, Roper JA, Martinez-Ramirez D, Opri E, Hess CW, Eisinger RS, Foote KD, Gunduz A, Okun MS. 2021. Closed-Loop Deep Brain Stimulation to Treat Medication-Refractory Freezing of Gait in Parkinson's Disease. *Front Hum Neurosci* **15**. doi:10.3389/fnhum.2021.633655

Neumann W, Rodriguez-Oroz MC. 2021. Machine Learning Will Extend the Clinical Utility of Adaptive Deep Brain Stimulation. *Movement Disorders* **36**:796–799. doi:10.1002/mds.28567

Neumann W-J, Degen K, Schneider G-H, Brücke C, Huebl J, Brown P, Kühn AA. 2016. Subthalamic synchronized oscillatory activity correlates with motor impairment in patients with Parkinson's disease. *Movement Disorders* **31**:1748–1751. doi:10.1002/mds.26759

Neumann W-J, Turner RS, Blankertz B, Mitchell T, Kühn AA, Richardson RM. 2019. Toward Electrophysiology-Based Intelligent Adaptive Deep Brain Stimulation for Movement Disorders. *Neurotherapeutics* **16**:105–118. doi:10.1007/s13311-018-00705-0

Neumann W-JJ, Schroll H, de Almeida Marcelino AL, Horn A, Ewert S, Irmen F, Krause P, Schneider G-HH, Hamker F, Kühn AA. 2018. Functional segregation of basal ganglia pathways in Parkinson's disease. *Brain* **141**:2655–2669. doi:10.1093/brain/awy206

Opri E, Cernera S, Molina R, Eisinger RS, Cagle JN, Almeida L, Denison T, Okun MS, Foote KD, Gunduz A. 2020. Chronic embedded cortico-thalamic closed-loop deep brain stimulation for the treatment of essential tremor. *Science translational medicine* **12**. doi:10.1126/scitranslmed.aay7680

Pernet C, Wilcox R, Rousselet G. 2013. Robust Correlation Analyses: False Positive and Power Validation Using a New Open Source Matlab Toolbox. *Frontiers in Psychology* **3**:606. doi:10.3389/fpsyg.2012.00606

Petrucci MN, Neuville RS, Afzal MF, Velisar A, Anidi CM, Anderson RW, Parker JE, O'Day JJ, Wilkins KB, Bronte-Stewart HM. 2020. Neural closed-loop deep brain stimulation for freezing of gait. *Brain Stimul* **13**:1320–1322. doi:10.1016/j.brs.2020.06.018

Piña-Fuentes D, van Dijk JMC, M B. 2019. Adaptive DBS in Parkinson's disease: Headlines, perspectives and challenges. *Brain Stimulation* **12**:1091–1092. doi:10.1016/j.brs.2019.04.014

Randazzo MJ, Kondylis ED, Alhourani A, Wozny TA, Lipski WJ, Crammond DJ, Richardson RM. 2016. Three-dimensional localization of cortical electrodes in deep brain stimulation surgery from intraoperative fluoroscopy. *Neuroimage* **125**:515–521. doi:10.1016/j.neuroimage.2015.10.076

Schwerdt HN, Amemori K, Gibson DJ, Stanwicks LL, Yoshida T, Bichot NP, Amemori S, Desimone R, Langer R, Cima MJ, Graybiel AM. 2020. Dopamine and beta-band oscillations differentially link to striatal value and motor control. *Science Advances* **6**:eabb9226. doi:10.1126/sciadv.abb9226

Shah SA, Tan H, Tinkhauser G, Brown P. 2018. Towards Real-Time, Continuous Decoding of Gripping Force From Deep Brain Local Field Potentials. *IEEE transactions on neural systems and rehabilitation engineering : a publication of the IEEE Engineering in Medicine and Biology Society* **26**:1460–1468. doi:10.1109/TNSRE.2018.2837500

Starr PA. 2018. Totally Implantable Bidirectional Neural Prostheses: A Flexible Platform for Innovation in Neuromodulation. *Front Neurosci* **12**. doi:10.3389/fnins.2018.00619

Swann NC, de Hemptinne C, Thompson MC, Miocinovic S, Miller AM, Gilron R, Ostrem JL, Chizeck HJ, Starr PA. 2018. Adaptive deep brain stimulation for Parkinson's disease using motor cortex sensing. *J Neural Eng* **15**:046006. doi:10.1088/1741-2552/aabc9b

Tan H, Pogosyan A, Ashkan K, Green AL, Aziz T, Foltynie T, Limousin P, Zrinzo L, Hariz M, Brown P. 2016. Decoding gripping force based on local field potentials recorded from subthalamic nucleus in humans. *Elife* **5**. doi:10.7554/eLife.19089

Tinkhauser G, Pogosyan A, Little S, Beudel M, Herz DM, Tan H, Brown P. 2017. The modulatory effect of adaptive deep brain stimulation on beta bursts in Parkinson's disease. *Brain* **140**:1053–1067. doi:10.1093/brain/awx010

Torrecillos F, Tinkhauser G, Fischer P, Green AL, Aziz TZ, Foltynie T, Limousin P, Zrinzo L, Ashkan K, Brown P, Tan H. 2018. Modulation of Beta Bursts in the Subthalamic Nucleus Predicts Motor Performance. *J Neurosci* **38**:8905–8917. doi:10.1523/JNEUROSCI.1314-18.2018

Turner RS, Desmurget M. 2010. Basal ganglia contributions to motor control: a vigorous tutor. *Curr Opin Neurobiol* **20**:704–716. doi:10.1016/j.conb.2010.08.022

Velisar A, Syrkin-Nikolau J, Blumenfeld Z, Trager MH, Afzal MF, Prabhakar V, Bronte-Stewart H. 2019. Dual threshold neural closed loop deep brain stimulation in Parkinson disease patients. *Brain Stimulation* **12**:868–876. doi:10.1016/j.brs.2019.02.020

Xie Z, Schwartz O, Prasad A. 2018. Decoding of finger trajectory from ECoG using deep learning. *J Neural Eng* **15**:036009. doi:10.1088/1741-2552/aa9dbe

Yttri EA, Dudman JT. 2016. Opponent and bidirectional control of movement velocity in the basal ganglia. *Nature* **533**:402–406. doi:10.1038/nature17639